Selected paper from 7th National Congress on Civil Engineering

Journal of Hydrosciences and Environment

ISSN: 2345-5608

Flood Wave Simulation Case Study for Natural Water Stream by Numerical Solutions of Unsteady Equations

P.Mirzazadeh*[1], Gh.Akbari[2]

1. P.G Researcher, University of Sistan and Baluchestan, Zahedan, Iran

2. Assoc. Prof. Civil Eng., Faculty of Eng., University of Sistan and Baluchestan, Zahedan, Iran

ARTICLE INFO

Article history:

Received: 3 May 2023
Accepted: 8 May 2023

Keywords:
Numerical Method
Saint-Venant
Priessmann ,
Lax
MIKE 11

A B S T R A C T

Modeling of river conditions and flood routing operations by numerical methods show a high accuracy.The beginning of the modern study of unsteady flow in open channels can be traced to the latter half of the nineteenth century when the French engineer Saint-Venant introduced the partial differential equations of continuity and momentum governing free surface flow in open channels. These equations are highly nonlinear and therefore do not have analytical solutions. This paper present the results of two different numerical methods, namely; Preissmann and Lax diffusive schemes for numerical solution of Saint-Venant equations that govern the propagation of flood wave, in natural rivers, with the objective of the better understanding of this propagation process. The results have shown that the hydraulic parameters play important game in the flood wave propagation. The results of these numerical solutions are compared with the MIKE.11 commercial computer model.

.

1. Introduction

Accomplished flood routing with mathematical methods helps designers to recognize flood effects on river rout and its surroundings. In unsteady open channel flows, the velocity and water depth change with time and longitudinal position. For one-dimensional applications, the relevant flow parameters (e.g., V and y) are functions of time and longitudinal distance. Flood wave propagation in overland and open channel flow may be described by the complete equations of motion for unsteady non uniform flow, known as the dynamic wave equations, first proposed by Saint-Venant in 1871[1]. These equations are nonlinear and therefore do not have analytical solutions. With the greatly improved speed and capacity of digital computers in recent years, dynamic routing models have been widely used for flood forecasting. The first major mathematical model of a river system was developed by J.J. Stoker for the Ohio and Mississippi systems. There have been numerous studies in the literature to solve the Saint-Venant equations by using different numerical techniques. In this research solution of the fully Saint-Venant equations through Lax diffusive explicit scheme and Preissmann implicit scheme for unsteady flow simulation in open channels is presented.

*Corresponding author's email: tezfeatures@gmail.com

2.Materials and Methods

2.1. Governing equation

The dynamic routing model is based on the dynamic wave theory of the Saint-Venant equations which consist of the continuity and momentum equations. The continuity and momentum equations defined as (no lateral inflow or outflow) [2]:

$$\frac{\partial A}{\partial t}+\frac{\partial Q}{\partial x}=0 \quad \text{(Continuity equation)} \qquad (1)$$

$$\frac{\partial y}{\partial t}+D_h\frac{\partial v}{\partial x}+V\frac{\partial y}{\partial x}=0 \qquad (2)$$

$$\frac{\partial Q}{\partial t}+\frac{\partial}{\partial x}(\beta QV)+gA\frac{\partial y}{\partial x}+gAS_f-gAS_0=0 \qquad (3)$$

where A is flow area, V is flow velocity, y is flow depth ,Q is discharge, B is top water surface width, Dh= A/B is hydraulic depth, t is time and x is distance along the channel length. β is the momentum correction factor, V is the cross-section average velocity g is the acceleration due to gravity, y is the flow depth, S0 is the channel longitudinal slope and Sf is slope of the energy grade line.

2.2. Model development and methodology

The continuity and momentum equations form a set of nonlinear hyperbolic partial differential equations. A closed form solution of these equations is not available except for very simplified cases. Therefore, numerical methods are used for their integration. The numerical solution of Eqs.1 and 2 can be obtained if appropriate initial and boundary conditions are prescribed. In this work, the fully Saint-Venant equations are solved for a rectangular wide river with 78 km length using Lax diffusive explicit scheme and four-point Preissmann implicit finite difference scheme. The results of these numerical solutions are compared with the MIKE.11commercial computer model.

2.3. Lax diffusive scheme

We have divided the x-t plane into a grid that the grid interval along the x-axis is Δx and the grid interval along the t-axis is Δt, we are assuming the grid size is uniform along each axis, although it is not necessary to do so. For brevity, we will call the iΔx grid point i and the (i + 1)Δx grid point i + 1. For the time axis, we will use k for kΔt grid point and k + 1 for the (k + 1)Δt grid point. To refer the different variables at these grid points, we will use the number of the spatial grid as a subscript and that of the time grid as a superscript. We will denote the known time level by superscript k and the unknown time level by k + 1.
To solve the Saint Venant equations, we may select the following finite difference approximations:

$$\frac{\partial f}{\partial x}=\frac{f_{i+1}^{k}-f_{i-1}^{k}}{2\Delta x} \qquad (4)$$

$$\frac{\partial f}{\partial t}=\frac{f_{i}^{k+1}-f_{i}^{k}}{\Delta t} \qquad (5)$$

This finite-difference scheme is inherently unstable. Lax presented a slight variation of the unstable scheme. This scheme is one of the simplest to program and yields satisfactory results for typical engineering applications. In this scheme the partial derivatives and other variables are approximated as follows [2]:

$$\frac{\partial f}{\partial x}=\frac{f_{i+1}^{k}-f_{i-1}^{k}}{2\Delta x} \qquad (6)$$

$$\frac{\partial f}{\partial t}=\frac{f_{i}^{k+1}-f^{*}}{\Delta t} \qquad (7)$$

$$f^{*}=\frac{\left(f_{i-1}^{k}+f_{i+1}^{k}\right)}{2} \qquad (8)$$

$$D^{*}=\frac{\left(D_{i-1}^{k}+D_{i+1}^{k}\right)}{2} \qquad (9)$$

$$S_f^{*}=\frac{\left(S_{f_{i-1}}^{k}+S_{f_{i+1}}^{k}\right)}{2} \qquad (10)$$

Where, for brevity, we are using f for both dependent variables, y and V. We use these approximations in the conservation forms of the governing equations as follows. The conservation form of the governing equations in the matrix form may be written as

$$U_t+F_x+S=0 \qquad (11)$$

In which

$$U=\begin{pmatrix}A\\VA\end{pmatrix};\ F=\begin{pmatrix}VA\\V^2A+gA\bar{y}\end{pmatrix};\ S=\begin{pmatrix}0\\-gA(S_0-S_f)\end{pmatrix} \qquad (12)$$

And $A\bar{y}$ is moment of flow area about the free surface. Substitution of the finite-difference approximations of Eqs.6,7,8,9 and 10 into Eq.11 yields

$$U_i^{k+1}=\frac{\left(U_{i+1}^{k}+U_{i-1}^{k}\right)}{2}-\frac{\left(F_{i+1}^{k}-F_{i-1}^{k}\right)\Delta t}{2\Delta x}-S^{*}\Delta t \qquad (13)$$

Once the values of A and VA have been determined at the (k+1) time level, we determine the values of variables of interest, y and V, and then proceed to the next time step.

2.4. Preissmann implicit scheme

Several implicit finite-difference schemes have been used for the analysis of unsteady open-channel flows [3,6]. The Preissmann scheme has been extensively used since the early 1960s [7].

The partial derivatives and other coefficients in this method are approximated as follows [2]:

$$\frac{\partial f}{\partial x} = \frac{\beta\left(f_{i+1}^{k+1} - f_i^{k+1}\right) + (1-\beta)\left(f_{i+1}^{k} - f_i^{k}\right)}{\Delta x} \qquad (14)$$

$$\frac{\partial f}{\partial t} = \frac{\left(f_i^{k+1} + f_{i+1}^{k+1}\right) - \left(f_i^{k} + f_{i+1}^{k}\right)}{\Delta x} \qquad (15)$$

$$f = \frac{1}{2}\,\beta\left(f_{i+1}^{k+1} + f_i^{k+1}\right) + \frac{1}{2}\,(1-\beta)\left(f_{i+1}^{k} + f_i^{k}\right) \qquad (16)$$

Where **β** is a weighting coefficient; f refers to both V and y in the partial derivatives, and f stands for S_f, and V as a coefficient. By selecting a suitable value for , the scheme may be made totally explicit (**β** = 0) or implicit (**β** = 1).
By substituting the above finite-difference approximations and the coefficients into Eq. 11, and rearranging the terms of the resulting equation, we obtain

$$U_i^{k+1} + U_{i+1}^{k+1} + 2\frac{\Delta t}{\Delta x}\cdot\left(\beta\left(F_{i+1}^{k+1} - F_i^{k+1}\right) + (1-\beta)\left(F_{i+1}^{k} - F_i^{k}\right)\right) + \Delta t\left(\beta\left(S_i^{k+1} + S_{i+1}^{k+1}\right) + (1-\beta)\left(S_{i+1}^{k} + S_i^{k}\right)\right) = U_i^{k} + U_{i+1}^{k} \qquad (17)$$

We have four unknowns, namely, U_i^{k+1} , A_i^{k+1} , U_{i+1}^{k+1} and A_{i+1}^{k+1} . If we write these two equations for each grid point, we have 2n equations (n = number of reaches on the channel). We cannot write these equations for the downstream end. However, we have 2(n+1) unknowns, i.e., two unknowns for each grid point. Thus, for a unique solution we need two more equations. These are provided by the boundary conditions. By applying the Eq.17 for each node and the boundary conditions we have a set of nonlinear algebraic equations. Here, the nonlinear equations have been solved by Newton-Raphson method.

2.5. Field evaluation model

Kor River is located in Fars province, Iran. The river is formed by branches of Tange Boragh and Shoor va Shirin and flows to Dorudzan Dam. Then the spill water join many other branches and sub-branch and enters Bakhtegan Lake after crossing a 200 km distance. In this study, the Sivand River data are used.

2.6. Initial and boundary conditions

Values of depth(y) and discharge(Q) at the beginning of the time step are to be specified at all the nodes along the channel as initial conditions. The two boundary conditions required by the model are the inflow discharge hydrograph at the upstream boundary, and the zero-depth at the downstream boundary. In the Lax diffusive explicit scheme, the Eq.13 may be used at the interior grid points to compute the unsteady flow depth and flow velocity. At the boundaries, however, we cannot use these equations, since there is no grid point outside the flow domain. In this procedure, for explicit schemes we solve the positive characteristic equation simultaneously with the condition imposed by the boundary for the downstream-end condition and the negative characteristic equation with the upstream-end condition for the upstream boundary[2]. Unlike the explicit schemes, we include directly in the system of equations the equations describing the end conditions. In other words, we do not have to use the characteristic equations or the reflection procedures.
This is one of the main advantages of the implicit schemes.
Since the flow regime is subcritical, a boundary condition in the upstream and a boundary condition in the downstream are required. In this study, the relationship between discharge-water levels is used as the downstream boundary condition. Also, the flood hydrograph with different return periods is considered as the upstream boundary condition. To this end, maximum discharge recorded at Chamriz station for a period of 35 years was collected. To obtain the discharge for different return periods, SAMADA software was used. After fitting different distributions, log Pearson type III was selected as the best distribution. Then, the discharge was calculated for return periods of 10, 25, 50 and 200 years and flood hydrographs for each peak discharge were obtained after deduction of Base Discharge using Soil Conservation Service (SCS) method. After obtaining this hydrograph, the base discharge was added to it. The hydrograph peak made in this way for each return period was the same as values obtained from SAMADA. It is noted that other physical information in a reach of 78 km length of Sivand River is shown in Table 1.

Table.1- River characteristic in studied reach

Reach (KM)	B (m)	S_0	n
0 - 20	**243**	**0.00027**	**0.033**
20 - 40	**217**	**0.00067**	**0.034**
40 - 78	**164**	**0.00051**	**0.037**

2.7. Stability

For the stability of explicit schemes, it is necessary that the Courant number, C_n, is less than or equal to 1, where

$$C_n = \frac{|V| \pm \sqrt{gy}}{\Delta x/\Delta t} \qquad (18)$$

Thus, the computational time interval depends upon the spatial grid spacing, flow velocity, and celerity, which are functions of the flow depth. Since the flow depth and the flow velocity may change significantly during the computations, it may be necessary to reduce the size of computational time interval for stability.

Courant condition must be satisfied at each grid point during every computational interval. The preissmann scheme is unconditionally stable provided 0.5≤**β**≤1, i.e., the flow variables are weighted towards the k + 1 time level[2].

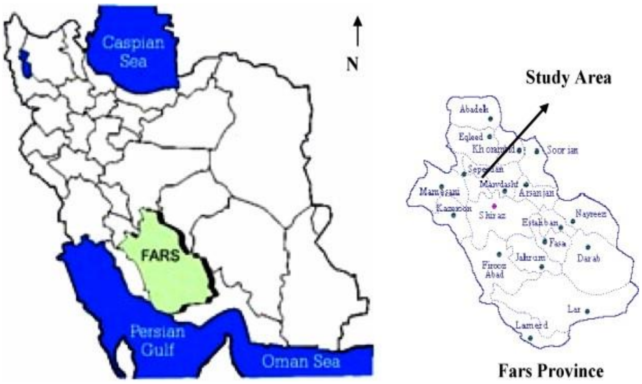

Fig.1. Geographic position of Kor and Sivand rivers in the study reaches.

2.8. Application of models

These models are applied to simulate hypothetical flood routing problems in a wide rectangular river. The results are compared to the MIKE.11 computer model.

2.9. Method of solution

For the Lax diffusive scheme, From the known initial conditions and using the discretized governing equations (Eq. 13) and by solution the positive characteristic equation simultaneously with the downstream- end boundary condition and the negative characteristic equation with the upstream-end boundary condition, the values of V and A, are obtained at all the nodes[2]. For Preissmann implicit scheme using the Separating governing equations (Eq.17) for each grid point, we have 2n equations (n = number of reaches on the channel that is here equal to 78). We cannot write these equations for the downstream. However, we have 2(n+1) unknowns, i.e., two unknowns for each grid point. Where;

$$V_{i+1}^{K+1} A_1^{k+1} = Q_1^{k+1} \qquad (19)$$

And by using downstream-end boundary, we obtain

$$V_{n+1}^{k+1} = \frac{1}{n}\left(\frac{A_{n+1}^{k+1}}{\left(B+2\frac{A_{n+1}^{k+1}}{B}\right)}\right)^{2/3} .\ S_f^{\ 1/2} \qquad (20)$$

The system of equations (Eq. 17 for each node and the boundary conditions (Eqs. 20 and 21)) are a set of nonlinear algebraic equations with 2(n + 1) equations in 2(n + 1) unknowns. We have used the Newton-Raphson method for solving the nonlinear system of equations. In this method, we have

$$x_1^{p+1} = x_0^p - w^{-1}(x_0^p) f(x_0^p) \qquad (21)$$

Where x_1 is the column matrix of 60 unknowns (V and A for each grid points) in advanced time step; x_0^p is the column matrix of initial guess for the unknown parameters, where the superscript p is the number of iterations (p=0, 1, 2,…); w is the jacobian square matrix of function that are generated from Eq. 17,19 and 23; f is the column matrix of functions that are generated from Eq. 17,19 and 20. Thus, the matrix form of Eq.21 may be written as

$$x_1^{p+1} = \begin{pmatrix} V_1^{k+1} \\ A_1^{k+1} \\ V_2^{k+1} \\ A_2^{k+1} \\ \vdots \\ \vdots \\ V_{n+1}^{k+1} \\ A_{n+1}^{k+1} \end{pmatrix};\ x_0^p = \begin{pmatrix} V_1^{k} \\ A_1^{k} \\ V_2^{k} \\ A_2^{k} \\ \vdots \\ \vdots \\ V_{n+1}^{k} \\ A_{n+1}^{k} \end{pmatrix};$$

$$\boldsymbol{f} = \begin{pmatrix} f_{\mathbf{1}}(\boldsymbol{V}_1^{k+1}, A_1^{k+1}) \\ f_{\mathbf{2}}(\boldsymbol{V}_1^{k+1}, A_1^{k+1}, \boldsymbol{V}_2^{k+1}, A_2^{\boldsymbol{k+1}}) \\ f_{\mathbf{3}}(\boldsymbol{V}_1^{k+1}, A_1^{k+1}, \boldsymbol{V}_2^{k+1}, A_2^{\boldsymbol{k+1}}) \\ f_{\mathbf{4}}(\boldsymbol{V}_2^{k+1}, A_2^{k+1}, \boldsymbol{V}_3^{k+1}, A_3^{\boldsymbol{k+1}}) \\ f_{\mathbf{5}}(\boldsymbol{V}_2^{k+1}, A_2^{k+1}, \boldsymbol{V}_3^{k+1}, A_3^{\boldsymbol{k+1}}) \\ \vdots \\ \vdots \\ f_{\mathbf{2n}}(\boldsymbol{V}_n^{k+1}, A_n^{k+1}, \boldsymbol{V}_{n+1}^{k+1}, A_{n+1}^{\boldsymbol{k+1}}) \\ f_{\mathbf{2n+1}}(\boldsymbol{V}_n^{k+1}, A_n^{k+1}, \boldsymbol{V}_{n+1}^{k+1}, A_{n+1}^{\boldsymbol{k+1}}) \\ f_{\mathbf{2n+2}}(\boldsymbol{V}_{n+1}^{k+1}, A_{n+1}^{k+1}) \end{pmatrix}$$

$$w = \begin{pmatrix} \frac{\partial f_1}{\partial v_1} & \frac{\partial f_1}{\partial A_1} & \frac{\partial f_1}{\partial v_2} & \frac{\partial f_1}{\partial A_2} & \cdots & \frac{\partial f_1}{\partial v_{n+1}} & \frac{\partial f_1}{\partial A_{n+1}} \\ \frac{\partial f_2}{\partial v_1} & \frac{\partial f_2}{\partial A_1} & \frac{\partial f_2}{\partial v_2} & \frac{\partial f_2}{\partial A_2} & \cdots & \frac{\partial f_2}{\partial v_{n+1}} & \frac{\partial f_2}{\partial A_{n+1}} \\ \frac{\partial f_3}{\partial v_1} & \frac{\partial f_3}{\partial A_1} & \frac{\partial f_3}{\partial v_2} & \frac{\partial f_3}{\partial A_2} & \cdots & \frac{\partial f_3}{\partial v_{n+1}} & \frac{\partial f_3}{\partial v_{n+1}} \\ \vdots & \vdots & \vdots & \vdots & & \vdots & \vdots \\ \frac{\partial f_{2n+1}}{\partial v_1} & \frac{\partial f_{2n+1}}{\partial A_1} & \frac{\partial f_{2n+1}}{\partial v_2} & \frac{\partial f_{2n+1}}{\partial A_2} & \cdots & \frac{\partial f_{2n+1}}{\partial v_{n+1}} & \frac{\partial f_{2n+1}}{\partial A_{n+1}} \\ \frac{\partial f_{2n+2}}{\partial v_1} & \frac{\partial f_{2n+2}}{\partial A_1} & \frac{\partial f_{2n+2}}{\partial v_2} & \frac{\partial f_{2n+2}}{\partial A_2} & \cdots & \frac{\partial f_{2n+2}}{\partial v_{n+1}} & \frac{\partial f_{2n+2}}{\partial A_{n+1}} \end{pmatrix}$$

For generate the f matrix for upstream-end boundary we have

$$f_1 = V_1^{k+1} A_1^{k+1} - Q_1^{k+1} \qquad (22)$$

And for even value of subscript i from 2 to 2m-2 and subscript j from 1 to m (m is the number of cross sections), using the Eq.17 we obtain

$$fi = A_{j+1}^{k+1} + A_j^{k+1} + 2\frac{\Delta t}{\Delta x}\left[\beta\left(V_{j+1}^{k+1}A_{j+1}^{k+1} - V_j^{k+1}A_j^{k+1}\right) + (1-\beta)\left(V_{j+1}^{k}A_{j+1}^{k} - V_j^{k}A_j^{k}\right)\right] - A_{j+1}^{k} - A_j^{k} \qquad (23)$$

And for odd value of subscript i from 3 to 2m-1 and subscript j from 1 to m, using the Eq. 17 we obtain

$$fi = V_{j+1}^{k+1}A_{j+1}^{k+1} + V_j^{k+1}A_j^{k+1} + 2\frac{\Delta t}{\Delta x}\Bigg(\beta\left(V_{j+1}^{2k+1}A_{j+1}^{k+1} + g\frac{A_{j+1}^{2k+1}}{2B} - V_j^{2k+1}A_j^{k+1} - g\frac{A_j^{2k+1}}{2B}\right) + (1-\beta)\left(V_{j+1}^{k}A_{j+1}^{k} - V_j^{k}A_j^{k}\right) + (1-\beta)\left(V_{j+1}^{2k}A_{j+1}^{k} + g\frac{A_{j+1}^{2k}}{2B} - V_j^{2k}A_j^{k} - g\frac{A_j^{2k}}{2B}\right)\Bigg) + \Delta t\left(\boldsymbol{\beta}\left(-gA_1^{k+1}\left(S_0 - \frac{V_j^{2k+1}n^2\left(B+2\frac{A_j^{k+1}}{B}\right)^{4/3}}{\left(A_j^{k+1}\right)^{4/3}}\right) - gA_{j+1}^{k+1}\left(S_0 - \frac{V_{j+1}^{2k+1}n^2\left(B+2\frac{A_{j+1}^{k+1}}{B}\right)^{4/3}}{\left(A_{j+1}^{k+1}\right)^{4/3}}\right)\right) + (1-\beta)\left(-gA_j^{k}\left(S_0 - S_{f_i}^{k}\right) - g\right)A_{j+1}^{k}\left(S_0 - S_{f_{i+1}}^{k}\right)\right)\Big) - V_{j+1}^{k}A_{j+1}^{k} - V_j^{k}A_j^{k} \qquad (24)$$

And by using the Eq. 20 for downstream-end boundary, we have

$$f_{2n+2} = V_{2n+2}^{k+1} - \frac{1}{n}\frac{\left(A_{2n+1}^{k+1}\right)^{2/3}}{\left(B+2\frac{\left(A_{2n+1}^{k+1}\right)}{B}\right)^{2/3}}\left(S_f^{k+1}\right)^{1/2} \qquad (25)$$

Now, we check that : $\sum_{i=1}^{n+1}|\Delta A_i| + |\Delta V_i| \leq \varepsilon$, where ε is the specified tolerance. If the sum of the corrections is less than the specified tolerance, then we proceed to the next step after applying the correction. Otherwise, we apply the correction and iterate the procedure. Here, we take the tolerance equal to 10^{-4}. Note that matrix w contains a large enough percentage of zeros. In the MATLAB software, we can convert the matrix w to a column matrix using sparse command. We may utilize this fact while solving Eq.25, since a vector solution routine requires less storage and gives more accurate results.

3. Results and discussions

The initial condition for all of the models corresponds to uniform flow with discharge 20 m^3/s . Also, the friction Slope is computed using Manning`s equation with roughness coefficient n (according to Table.1).The upstream discharge hydrograph (Flood with different return period) and the downstream stage-discharge relationship are used as boundary conditions for the models. The computed unsteady flow data through numerical methods and MIKE.11 model at 70km section are given in table3.

To analyze the results of each method, Table 2 which shows values of flood flow peak properties at 7 spatial intervals and Table 2 that shows the changes in flood at Km +70.00 were used. Also, the discharge – depth curve shown in Figure 2 was used. One of the merits of the Preissmann implicit model is that it does not limit the choice of the time interval. Results showed that increase in the interval, slightly decreases rooted hydrograph peak discharge, but what is important is that selecting a big interval reduces the computation time without affecting the error rate. This is one of the advantages of Preissmann implicit model.Studies show that Lax pattern is highly sensitive to characteristics of the flood hydrograph (discharge and peak time) in the upstream reach. This pattern is not seen in Preissmann implicit model.

Also, the results seen in Table 2, indicates that results of Preissmann implicit model are very close to the solutions done by Mike11 software. There is a little difference which is due to energy equation being replaced by momentum equation in Preissmann implicit model. It is clear that the explicit Lax pattern estimates peak discharge values as being less than the other two models. However, Preissmann implicit model estimates peak discharge values slightly higher than the software results. This implies a higher assurance in calculating flood peak values for designers. For depth values Lax pattern predicts higher values less rapidly.

According to the above results, Preissmann implicit model is better than Lax pattern and is recommended because it provides a better safety margin with respect to flood routing operation.

Table.2. Obtained results in different section of the river

	Preissmann implicit scheme				Lax diffusive			
Distance From Upstream (Km)	Qp $\left(\frac{m^3}{sec}\right)$	tp $(hour)$	V_p $\left(\frac{m}{s}\right)$	y_p (m)	Qp $\left(\frac{m^3}{sec}\right)$	tp $(hour)$	V_p $\left(\frac{m}{s}\right)$	y_p (m)
+12.50	59.756	129.83	0.707	3.058	59.752	129.75	0.713	3.04
+25.00	59.694	132.66	1.146	2.588	59.690	132.58	1.146	2.58
+32.50	59.686	133.91	1.002	2.078	59.680	133.83	1.001	2.07
+45.00	59.661	137.25	0.554	1.007	59.644	137.16	0.554	1.00
+57.50	59.586	141.42	0.528	1.114	59.476	141.50	0.475	1.17
+70.00	57.399	150.33	0.229	1.974	57.005	150.33	0.222	2.00
+78.00	57.078	155.16	0.355	1.303	56.658	155.083	0.354	1.30

Fig.2. The curve of Discharge-Depth in Km +70.00

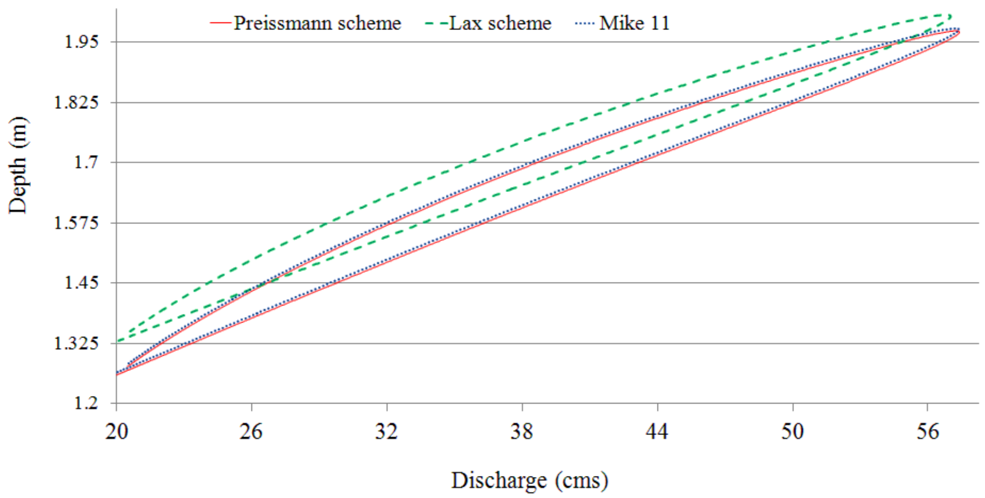

Table 3. Computed Velocity, Stage and Discharge hydrograph at 78 Km section using all of model

	70 Km from upstream end											
	Upstream-end		Preissmann			Lax diffusive			MIKE 11			
Time (hour)	Q (cms)	Y (m)	Q (cms)	Y (m)	V (m/s)	Q (cms)	Y (m)	V (m)	Q (cms)	Y (m)	V m/s
0	20	1.362	20	1.26	0.141	20	1.243	0.144	20	1.262	0.140
24	20.025	1.363	20.003	1.26	0.141	20	1.318	0.13	20	1.264	0.141
48	20.54	1.376	20.012	1.26	0.141	20	1.327	0.131	20.01	1.265	0.141
60	21.86	1.408	20.064	1.261	0.142	20.036	1.329	0.131	20.06	1.266	0.141
72	25.19	1.488	20.287	1.265	0.143	20.288	1.334	0.132	20.29	1.27	0.142
78	28.01	1.553	20.565	1.271	0.144	20.581	1.339	0.133	20.57	1.276	0.143
84	31.74	1.636	21.062	1.28	0.146	21.098	1.349	0.135	21.08	1.286	0.145
90	36.34	1.735	21.919	1.297	0.149	21.979	1.365	0.139	21.94	1.303	0.149
96	41.6	1.844	23.324	1.325	0.155	23.412	1.391	0.145	23.34	1.331	0.154
102	47.09	1.954	25.514	1.368	0.162	25.639	1.432	0.153	25.53	1.374	0.162
108	52.28	2.05	28.687	1.43	0.172	28.836	1.49	0.163	28.68	1.435	0.172
114	56.51	2.116	32.911	1.511	0.184	33.02	1.565	0.176	32.871	1.516	0.183
120	59.211	2.155	37.981	1.606	0.197	38.044	1.655	0.189	37.9	1.61	0.196
126	59.98	2.168	43.544	1.707	0.208	43.517	1.75	0.201	43.45	1.71	0.207
132	58.71	2.154	48.953	1.804	0.218	48.816	1.843	0.211	48.87	1.809	0.217
138	55.58	2.116	53.455	1.886	0.226	53.206	1.92	0.219	53.38	1.891	0.225
144	51.06	2.05	56.364	1.943	0.229	56.008	1.975	0.222	56.3	1.948	0.228
150	45.74	1.967	57.395	1.97	0.229	57.002	2.003	0.222	57.35	1.976	0.228
156	40.25	1.85	56.671	1.97	0.226	56.282	2.005	0.219	56.64	1.97	0.225
162	35.134	1.741	54.514	1.947	0.22	54.151	1.984	0.213	54.5	1.952	0.219
168	30.736	1.638	51.271	1.903	0.213	50.953	0.205	1.944	51.271	1.909	0.212
174	27.231	1.553	47.351	1.845	0.204	47.11	1.89	0.196	47.364	1.851	0.203
180	24.624	1.487	43.107	1.778	0.194	42.944	1.827	0.186	43.132	1.784	0.194
192	21.619	1.407	35.025	1.632	0.176	35.043	1.69	0.167	35.047	1.638	0.175
204	20.461	1.375	28.764	1.499	0.161	28.918	1.565	0.152	28.799	1.506	0.16
216	20.107	1.365	24.619	1.398	0.151	24.816	1.469	0.142	24.66	1.404	0.15
228	20.02	1.363	22.227	1.332	0.145	22.42	1.406	0.136	22.257	1.338	0.145
251	20	1.362	20.479	1.277	0.142	20.595	1.35	0.132	20.49	1.282	0.141

4. References

1. Saint-Venant, B. D. (1871). "Theory of unsteady water flow, with application to river floods and to propagation of tides in river channels." French Academy of Science, 73, 148–154, 37–240.

2. Chaudhry, MH. 1987. "Applied Hydraulic Transients." Van Nostrand Reinhold Company: New York.

3. Amein, M., and Fang. C. S.(1970)." Implicit flood routing in natural channel" J. Hydraul. Div., Am. Soc. Civ. Eng., 96(12), 2481–2500.

4. Liggett, J. A., and Cunge, J. A. (1975). "Numerical methods of solution of the unsteady flow equations in

open channels, K. Mahmood and V. Yevjevich, eds., Water Resources, Fort Collins, Colo., 89–182.

5. Abbott MB. 1979. “Computational Hydraulics.” Pitman: London.

6. Cunge J.A, Holly FM Jr, Verwey A. 1980. “ Practical Aspects of Computational River Hydraulics.” Pitman: London.

7. Preissmann, A., (1961). “Propagation of translatory waves in channels and rivers” Proc., 1st Congress of French Association for Computation,Grenoble, France, A. F. C. A. L., 433–442 (in French).

8. MIKE 11 a modeling system for Rivers and Channels, User’s Manual, 11 4.10.